C-type natriuretic peptide facilitates autonomous Ca^{2+} entry in growth plate chondrocytes for stimulating bone growth

C 型ナトリウム利尿ペプチドは
自発的な Ca^{2+} 流入を介して骨伸長を促進する

Graduate School of Pharmaceutical Sciences,
Kyoto University

宮﨑　侑

Contents

Abstract

The growth plates are cartilage tissues found at both ends of developing bones, and vital proliferation and differentiation of growth plate chondrocytes are primarily responsible for bone growth. C-type natriuretic peptide (CNP) stimulates bone growth by activating natriuretic peptide receptor 2 (NPR2) which is equipped with guanylate cyclase on the cytoplasmic side, but its signaling pathway is unclear in growth plate chondrocytes. I previously reported that transient receptor potential melastatin-like 7 (TRPM7) channels mediate intermissive Ca^{2+} influx in growth plate chondrocytes, leading to activation of Ca^{2+}/calmodulin-dependent protein kinase II (CaMKII) for promoting bone growth. In this report, I provide experimental evidence indicating a functional link between CNP and TRPM7 channels. My pharmacological data suggest that CNP-evoked NPR2 activation elevates cellular cGMP content and stimulates big-conductance Ca^{2+}-dependent K^+ (BK) channels as a substrate for cGMP-dependent protein kinase (PKG). BK channel-induced hyperpolarization likely enhances the driving force of TRPM7-mediated Ca^{2+} entry and seems to accordingly activate CaMKII. Indeed, *ex vivo* organ culture analysis indicates that CNP-facilitated bone growth is abolished by chondrocyte-specific *Trpm7* gene ablation. The defined CNP signaling pathway, the NPR2-PKG-BK channel-TRPM7 channel-CaMKII axis, likely pinpoints promising target proteins for developing new therapeutic treatments for divergent growth disorders.

Introduction

The development of skeletal long bones occurs through endochondral ossification processes, during which chondrocyte layers form the growth plates at both ends of bone rudiments, and then the expanded cartilage portions are gradually replaced by trabecular bones through the action of osteoclasts and osteoblasts [1]. Therefore, bone size largely depends on the proliferation of growth plate chondrocytes during endochondral development. On the other hand, atrial (ANP), brain (BNP) and C-type (CNP) natriuretic peptides regulate diverse cellular functions by activating the receptor guanylate cyclases, NPR1 and NPR2 [2]. Of the natriuretic peptides, CNP exclusively stimulates bone development by acting on growth plate chondrocytes expressing the CNP-specific receptor NPR2 [2-4]. Indeed, loss- and gain-of-function mutations in the human *NPR2* gene cause acromesomelic dysplasia and skeletal overgrowth disorder, respectively [5, 6]. Furthermore, translational studies have been probing the benefits of CNP treatments in various animal models with impaired skeletal growth, and a phase III clinical trial of CNP therapy has recently been completed and approved for treatment of patients with achondroplasia primarily resulting from mutations in the *FGFR3* gene [7]. It is thus likely that NPR2 guanylate cyclase controls chondrocytic cGMP content during growth plate development. Downstream of NPR2 activation, cGMP-dependent protein kinase (PKG) seems to phosphorylate target proteins to facilitate growth plate chondrogenesis [4]. Activated

PKG is postulated to stimulate the biosynthesis of growth plate extracellular matrix by playing an inhibitory role in the mitogen-activated protein kinase Raf-MEK-ERK cascade [8]. In parallel, glycogen synthase kinase 3β (GSK3β) is likely activated by PKG-mediated phosphorylation, leading to the hypertrophic maturation of growth plate chondrocytes [9]. However, it is still unclear how CNP promotes bone growth at the molecular level, and it is important to further address CNP signaling cascade in growth plate chondrocytes.

In the transient receptor potential channel superfamily, the melastatin subfamily member 7 (TRPM7) forms a mono- and divalent cation-permeable channel in various cell types and participates in important cellular processes including cell growth and adhesion [10]. My research group recently reported that growth plate chondrocytes generate autonomic intracellular Ca^{2+} fluctuations, which are generated by the intermittent gating of TRPM7 channels, and also that TRPM7-mediated Ca^{2+} entry activates Ca^{2+}/calmodulin-dependent protein kinase II (CaMKII), facilitating chondrogenesis for endochondral bone development [11]. Based on these observations, I explored the link between CNP signaling and TRPM7-mediated Ca^{2+} entry through the experiments described in this report. My data obtained clearly indicate that big-conductance Ca^{2+}-dependent K^+ (BK) channels play a key role in the functional coupling between NPR2 and TRPM7 channels in growth plate chondrocytes.

Results

CNP facilitates spontaneous Ca^{2+} fluctuations in growth plate chondrocytes

In the growth plates of developing bones, proliferating cartilage cells, designated as round and columnar chondrocytes, frequently exhibit weak increases and decreases in intracellular Ca^{2+} concentration under resting conditions [11]. On the other hand, previous *in vivo* studies demonstrated that CNP application (>1 μmol/kg) stimulates endochondral bone growth [2]. In my Fura-2 imaging of round chondrocytes within femoral bone slices prepared from wild-type mice, CNP pretreatments (30~300 nM for 1 hr) dose-dependently facilitated spontaneous Ca^{2+} fluctuations (Figure 1A). In particular, fluctuation-positive cell ratio and fluctuation amplitude were remarkably elevated in response to the CNP treatments. In contrast, ANP treatments exerted no effects on Ca^{2+} fluctuations in growth plate chondrocytes.

In chondrocyte-specific *Npr2*-knockout mice (*Npr2*$^{fl/fl}$, *Col2a1-Cre*$^{+/-}$), Cre recombinase is expressed under the control of the collagen type 2α1 gene promoter and thus inactivates the floxed *Npr2* alleles in a chondrocyte-specific manner [12]. My RT-PCR analysis indicated that the floxed *Npr2* gene was largely inactivated in the growth plates prepared from the E17.5 mutant embryos, but such recombination events were not detected in other tissues examined (Figure 2A and B). Accordingly, *Npr2* mRNA contents in the mutant growth plates were reduced to less than 40% of

controls (Figure 2C), despite the growth plate preparations contain not only chondrocytes but also perichondrium-resident cells including undifferentiated mesenchymal cells and immature chondroblasts. In contrast to the imaging observations in wild-type and control bone slices, CNP treatments failed to enhance Ca^{2+} fluctuations in the mutant round chondrocytes prepared from the chondrocyte-specific *Npr2*-knockout mice (Figure 1B). Therefore, CNP seems to facilitate spontaneous Ca^{2+} fluctuations downstream of NPR2 activation in growth plate chondrocytes.

Figure 1

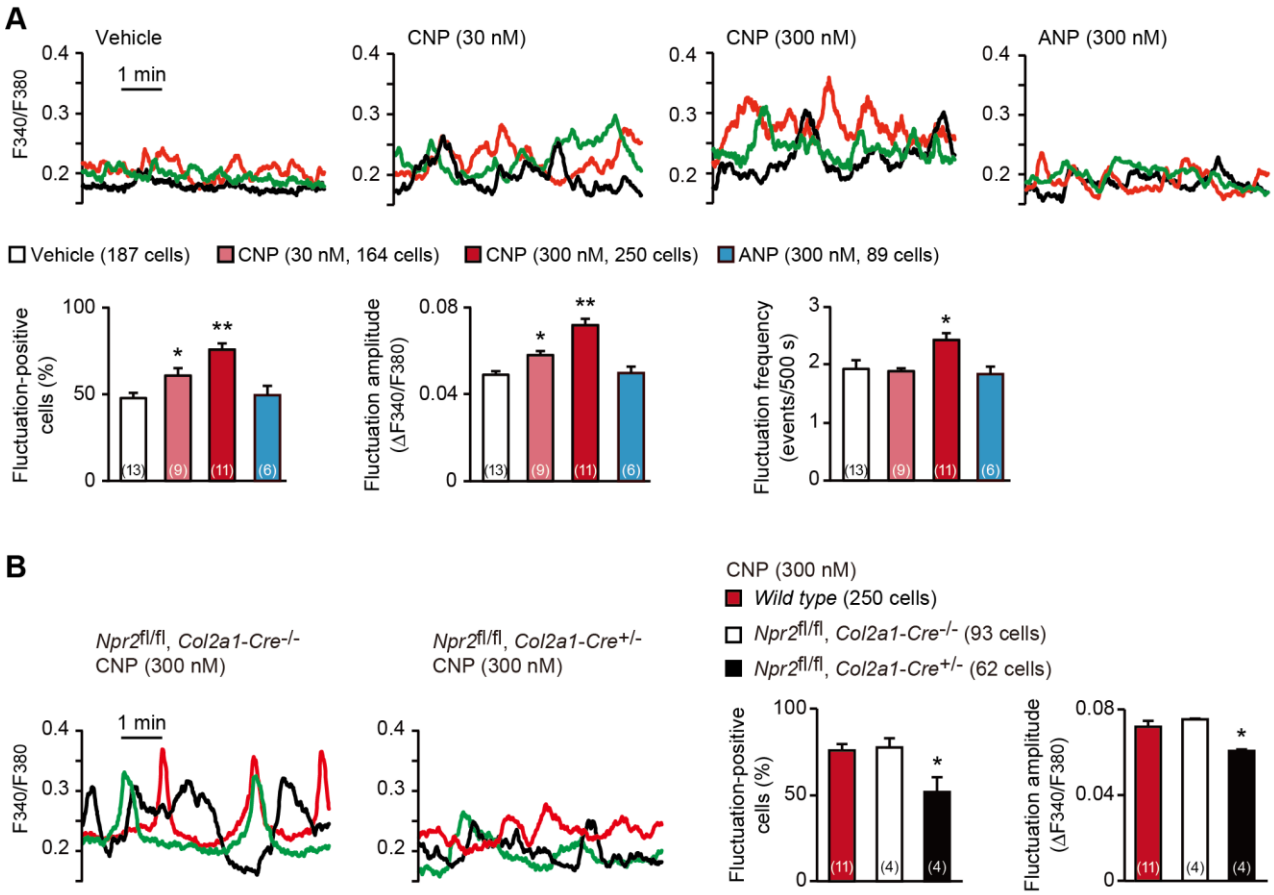

CNP-induced facilitation of Ca^{2+} fluctuations in growth plate chondrocytes.

(A) Fura-2 imaging of round chondrocytes pretreated with or without natriuretic peptides. Femoral bone slices prepared from wild-type C57BL embryos were pretreated with or without CNP and ANP, and subjected to Ca^{2+} imaging. Representative recording traces from three cells are shown in each pretreatment group (upper panels). The effects of CNP and ANP pretreatments on spontaneous Ca^{2+} fluctuations are summarized (lower graphs). The fluctuation-positive cell ratio, fluctuation amplitude and frequency were statistically analyzed, and significant differences from the control vehicle pretreatment are marked with asterisks (*p<0.05 and **p<0.01 in one-way ANOVA and Dunnett's test). The data are presented as the means ± SEM. with n values indicating the number of examined mice. **(B)** Fura-2 imaging of round chondrocytes prepared from chondrocyte-specific *Npr2*-knockout (*Npr2*$^{fl/fl}$, *Col2a1-Cre*$^{+/-}$) and control (*Npr2*$^{fl/fl}$, *Col2a1-Cre*$^{-/-}$) mice. The bone slices were pretreated with CNP, and then subjected to Ca^{2+} imaging. Representative recording traces are shown (left panels) and the CNP-pretreated effects are summarized (right graphs); significant differences from the wild-type group are marked with asterisks (*p<0.05 in one-way ANOVA and Tukey's test). The data are presented as the means ± SEM. with n values indicating the number of examined mice.

Figure 2

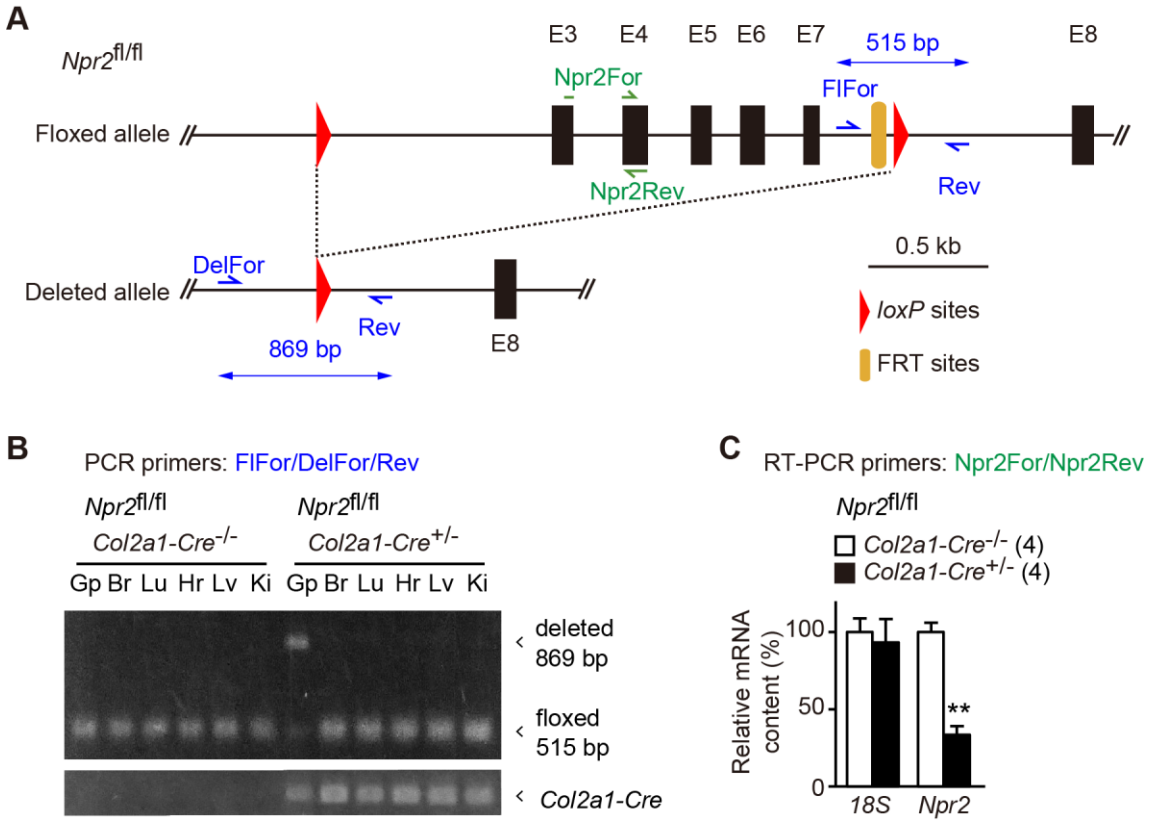

Chondrocyte-specific *Npr2* ablation.

(A) Organization of floxed and deleted *Npr2* alleles. The chondrocyte-specific *Npr2*-knockout (*Npr2*$^{fl/fl}$, *Col2a1-Cre*$^{+/-}$) mice were previously generated [12]. In this study, genotyping primers were newly designed, and *Npr2* ablation was evaluated in growth plates. The genomic map shows PCR primers for detecting the mutated *Npr2* alleles and *Npr2* mRNA. **(B)** *Npr2* gene ablation in various tissues from the chondrocyte-specific *Npr2*-knockout mice. Genomic DNAs were prepared from tissues (Gp, humeral growth plate; Br, brain; Lu, lung; Hr, heart; Lv, liver; Ki, kidney) from the E17.5 chondrocyte-specific *Npr2*-knockout and control embryos, and subjected to PCR analysis to detect the floxed and deleted *Npr2* alleles; the *Col2a1-Cre* transgene was also examined. **(C)** Reduction of *Npr2* mRNA in mutant growth plates prepared from the chondrocyte-specific *Npr2*-knockout mice. Total RNAs were prepared from humeral growth plates from the E17.5 embryos, and subjected to RT-PCR analysis for estimating *Npr2* mRNA content. 18S ribosomal RNA was examined as an internal control. The relative mRNA contents were estimated from cycle thresholds in RT-PCR reactions and are summarized in the bar-graph. The data represent means ± SEM, and the numbers of mice examined are shown in parentheses. A significant difference between the genotype is marked with an asterisk (**p<0.01 in t-test).

Activated PKG facilitates spontaneous Ca^{2+} fluctuations

CNP binds to NPR2 to activate its intrinsic guanylate cyclase and thus stimulates PKG by elevating cellular cGMP contents [2]. CNP also binds to NPR3 which acts as a decoy receptor for ligand clearance, but the *Npr3* gene seemed to be inactive in growth plate chondrocytes (Figure 3). Next, I pharmacologically verified the contribution of PKG to CNP-facilitated Ca^{2+} fluctuations. The cGMP analog 8-(4-chlorophenylthio)-cyclic GMP (8-pCPT-cGMP) is widely used as a PKG-selective activator, while KT5823 is a typical PKG inhibitor. In wild-type growth plate chondrocytes pretreated with 8-pCPT-cGMP (100 μM for 1 hr), spontaneous Ca^{2+} fluctuations were remarkably facilitated (Figure 4A); both fluctuation-positive cell rate and fluctuation amplitude were highly increased. In contrast, the bath application of KT5823 (2 μM) clearly attenuated CNP-facilitated Ca^{2+} fluctuations within a short time frame (Figure 4B). Therefore, PKG activation seems to be essential for CNP-facilitated Ca^{2+} fluctuations in growth plate chondrocytes.

Figure 3

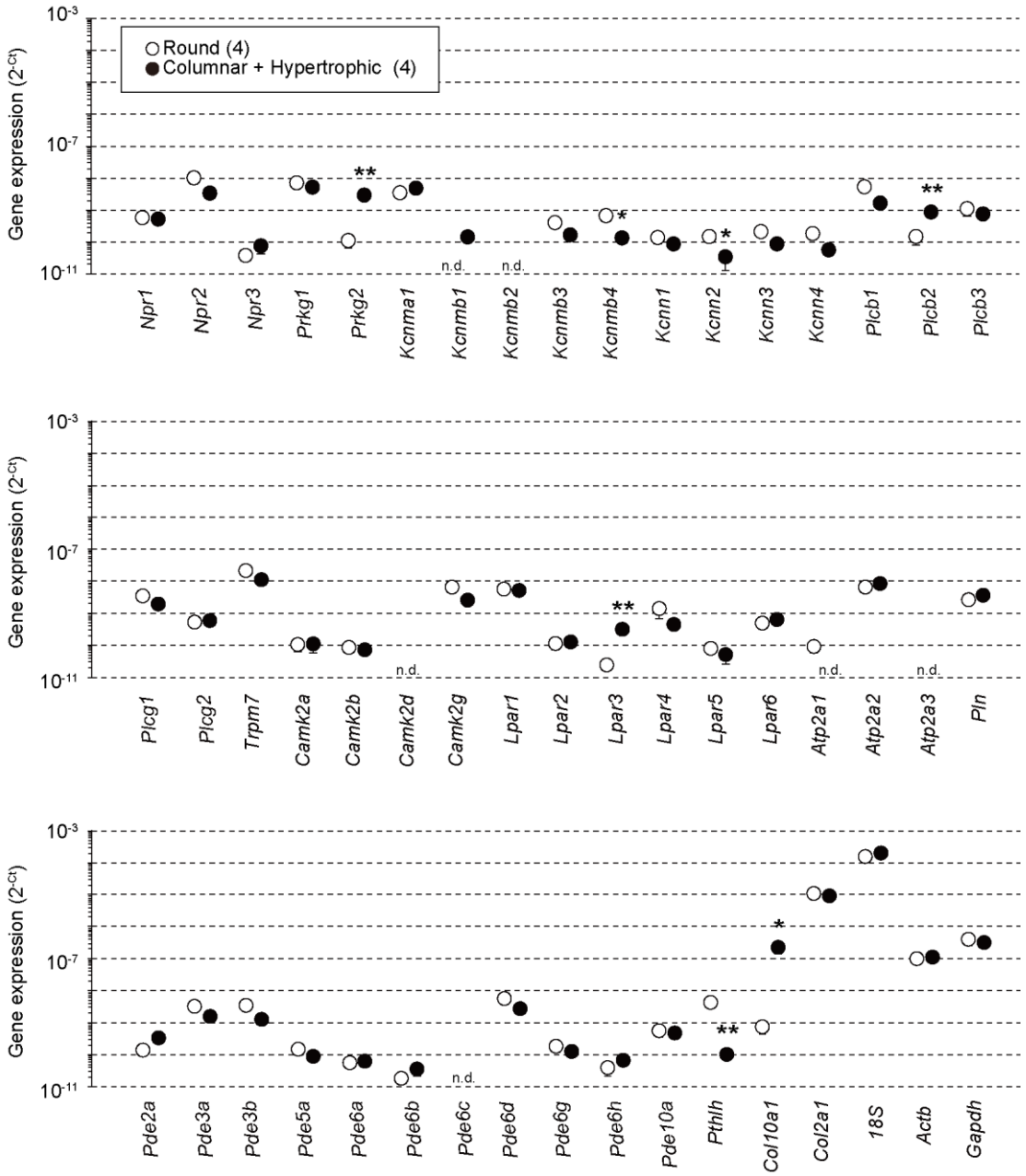

Gene expression analysis in wild-type growth plate chondrocytes.

Total RNAs were prepared from growth plate sections packed with round chondrocytes or enriched with columnar and hypertrophic chondrocytes, and subjected to RT-PCR analysis. The cycle threshold (Ct) was determined for each RT-PCR reaction for estimating relative mRNA content. The data represent the mean ± SEM, and the numbers of mice examined are shown in parentheses. Significant differences between the growth plate sections are marked with asterisks (*p<0.05 and **p<0.01 in t-test). n.d.: not detectable.

Figure 4

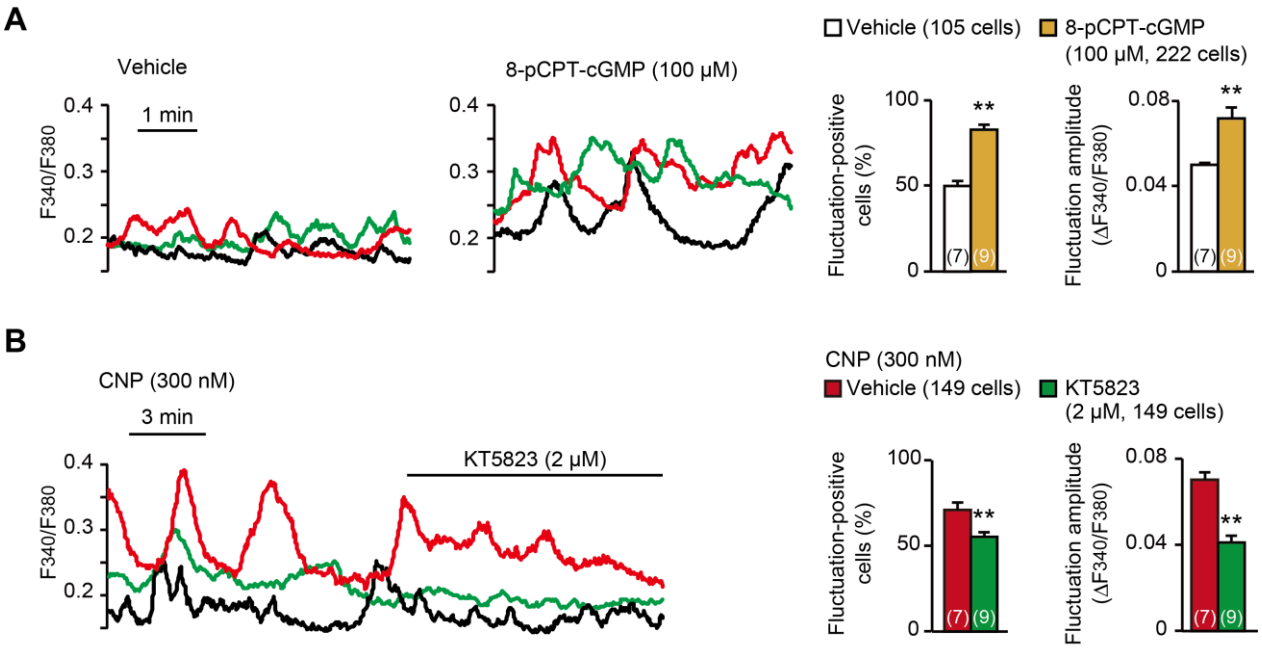

Contribution of PKG to CNP-facilitated Ca^{2+} fluctuations.

(A) Facilitated Ca^{2+} fluctuations in round chondrocytes pretreated with the PKG activator 8-pCPT-cGMP. Wild-type bone slices were pretreated with or without the cGMP analog, and then subjected to Ca^{2+} imaging. Representative recording traces are shown (left panels), and the pharmacological effects are summarized (right graphs). Significant differences between control and 8-pCPT-cGMP pretreatments are marked with asterisks (**p<0.01 in t-test). The data are presented as the means ± SEM. with n values indicating the number of examined mice. **(B)** Attenuation of CNP-facilitated Ca^{2+} fluctuations by the PKG inhibitor KT5823. Wild-type bone slices were pretreated with CNP, and then subjected to Ca^{2+} imaging. Representative recording traces are shown (left panel), and KT5823-induced effects are summarized (right graphs). Significant KT5823-induced shifts are marked with asterisks (**p<0.01 in t-test). The data are presented as the means ± SEM. with n values indicating the number of examined mice.

Activated BK channels contribute to CNP-facilitated Ca^{2+} fluctuations

Spontaneous Ca^{2+} fluctuations are facilitated by activated BK channels in growth plate chondrocytes [11]. Previous studies have established a functional link between PKG and BK channels in several cell types including smooth muscle and endothelial cells; activated PKG enhances BK channel gating by directly phosphorylating the α subunit KCNMA1 protein [13-15]. I thus examined whether altered BK channel activity is associated with CNP-facilitated Ca^{2+} fluctuations. The BK channel inhibitor paxilline (10 μM) exerted no obvious effects on basal Ca^{2+} fluctuations in non-treated chondrocytes. However, the same paxilline treatments remarkably inhibited CNP-facilitated Ca^{2+} fluctuations (Figure 5A); both fluctuation-positive cell ratio and fluctuation amplitude were clearly decreased after paxilline application. On the other hand, the BK channel activator NS1619 (30 μM) stimulated basal Ca^{2+} fluctuations in the growth plate chondrocytes prepared from control mice. The NS1619-induced effects were preserved in the mutant chondrocytes prepared from chondrocyte-specific *Npr2*-knockout mice (Figure 5B). Therefore, BK channel activation is likely involved in CNP-facilitated Ca^{2+} fluctuations in growth plate chondrocytes.

Figure 5

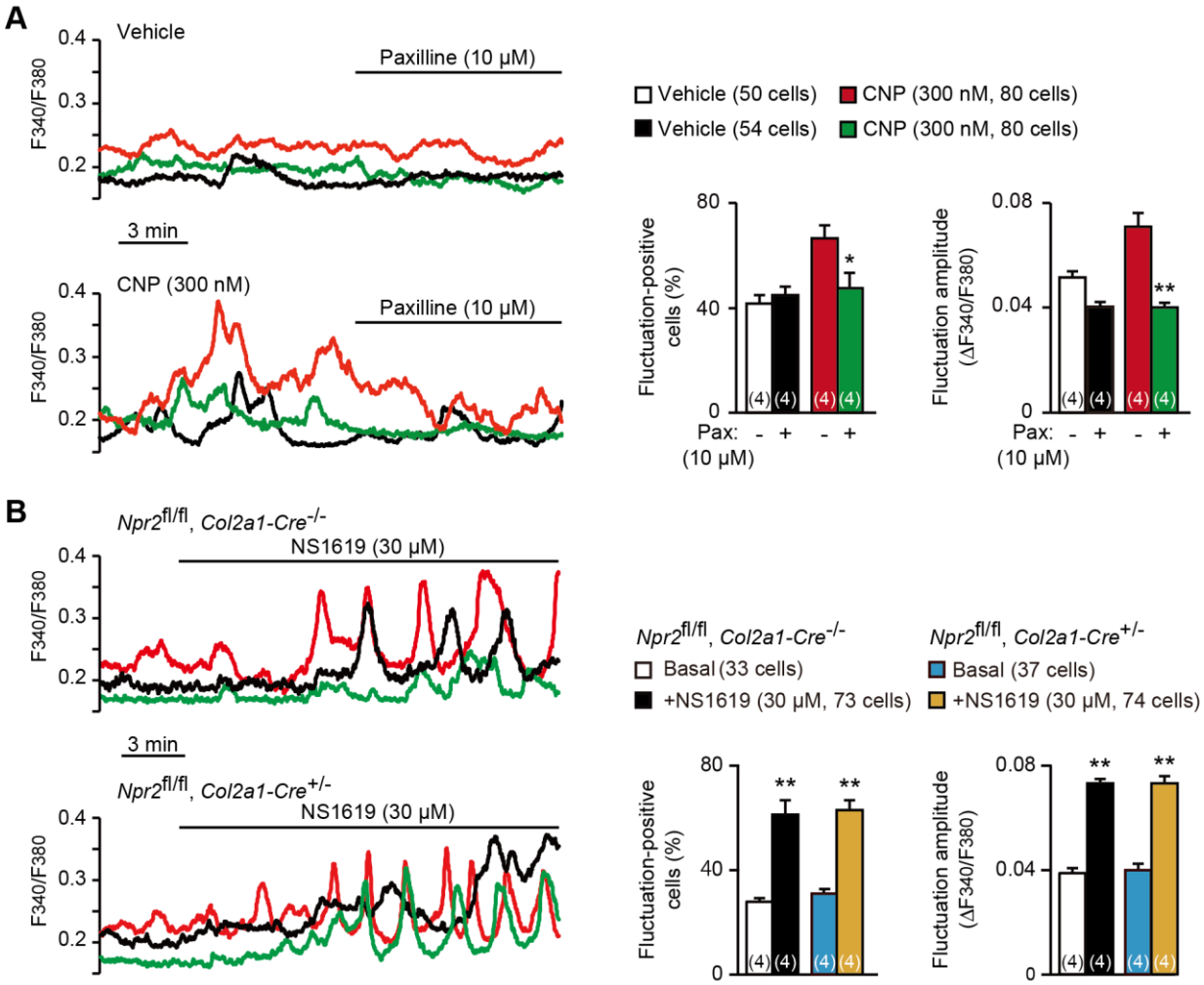

Contribution of BK channels to CNP-facilitated Ca^{2+} fluctuations.

(A) Attenuation of CNP-facilitated Ca^{2+} fluctuations by the BK channel inhibitor paxilline in round chondrocytes. Wild-type bone slices were pretreated with or without CNP, and then subjected to Ca^{2+} imaging. Representative recording traces are shown (left panels), and paxilline-induced effects are summarized (right graphs). Significant paxilline-induced shifts are marked with asterisks (*p<0.05 and **p<0.01 in one-way ANOVA and Tukey's test). The data are presented as the means ± SEM. with n values indicating the number of examined mice. **(B)** Ca^{2+} fluctuations facilitated by the BK channel activator NS1619 in *Npr2*-deficient chondrocytes. Bone slices were prepared from the chondrocyte-specific *Npr2*-knockout and control embryos, and NS1619-induced effects were examined in Ca^{2+} imaging. Representative recording traces are shown (left panels), and the effects of NS1619 are summarized (right graphs). Significant NS1619-induced shifts are marked with asterisks (**p <0.01 in one-way ANOVA and Tukey's test). The data are presented as the means ± SEM. with n values indicating the number of examined mice.

PLC seems unrelated to CNP-facilitated Ca^{2+} fluctuations

Ca^{2+} fluctuations are maintained by phosphatidylinositol (PI) turnover in growth plate chondrocytes [11]. Although it has been reported that activated PKG inhibits phospholipase C (PLC) in smooth muscle [16-19], it might be possible that NPR2 activation enhances basal PLC activity to facilitate Ca^{2+} fluctuations. The PLC inhibitor U73122 (10 μM) remarkably inhibited basal Ca^{2+} fluctuations in non-treated chondrocytes: the fluctuation-positive cell ratio and fluctuation amplitude reduced less than half in response to U73122 application (Figure 6). U73122 was also effective for CNP-facilitated Ca^{2+} fluctuations, but the inhibitory efficiency seemed relatively weak compared to those on basal fluctuations. Given the different inhibitory effects, it is rather unlikely that PLC activation accompanies CNP-facilitated Ca^{2+} fluctuations.

PKG stimulates sarco/endoplasmic reticulum Ca^{2+}-ATPase (SERCA) by phosphorylating the Ca^{2+} pump regulatory peptide phospholamban (PLN) in smooth and cardiac muscle cells [20-22], and activated Ca^{2+} pumps generally elevate stored Ca^{2+} content and thus stimulate store Ca^{2+} release. RT-PCR data suggested that the *Pln* gene and the *Atp2a2* gene encoding SERCA2 are weakly active in growth plate chondrocytes (Figure 3). To examine the effects of CNP treatments on Ca^{2+} stores, I examined Ca^{2+} responses to the activation of Gq-coupled lysophosphatidic acid (LPA) receptors (Figure 7A) and the Ca^{2+} pump inhibitor thapsigargin (Figure 7B). CNP- and vehicle-pretreated

chondrocytes exhibited similar LPA-induced Ca^{2+} release and thapsigargin-induced Ca^{2+} leak responses. Therefore, CNP treatments seem ineffective for store Ca^{2+} pumps in growth plate chondrocytes. Moreover, the dose-dependency of Ca^{2+} release by LPA (1~10 μM) was not altered between CNP- and vehicle-pretreated chondrocytes, implying that CNP does not affect basal PLC activity.

Among diverse Ca^{2+} handling-related proteins, PLC, PLN and BK channels have been reported as PKG substrates, however, my observations suggested that both PLC and PLN receive no obvious functional regulation in CNP-treated chondrocytes. On the other hand, the paxilline treatments diminished CNP-facilitated Ca^{2+} fluctuations down to non-treated control levels (Figure 5A), suggesting that activated BK channels predominantly contribute to CNP-facilitated Ca^{2+} fluctuations in growth plate chondrocytes.

Figure 6

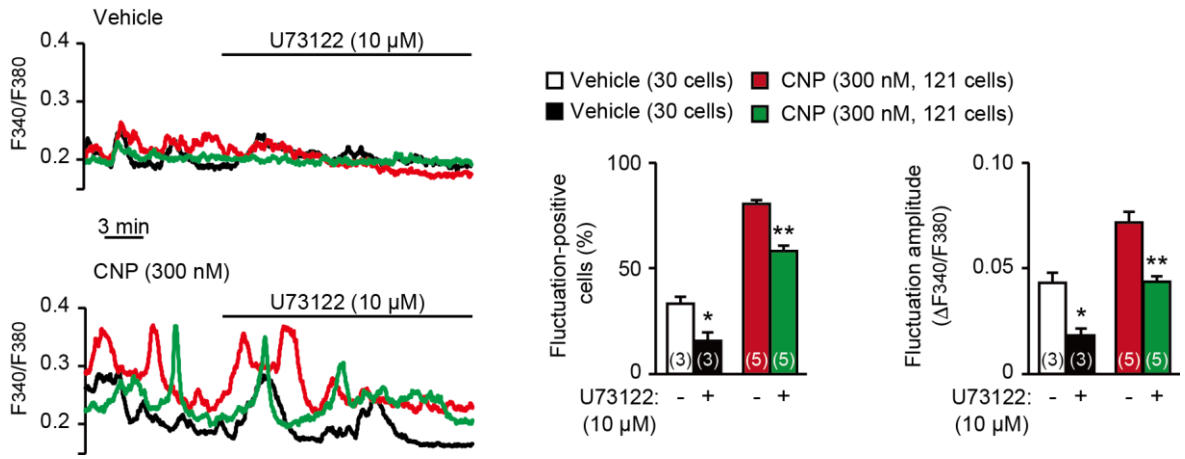

Effects of PLC inhibitor U73122 on CNP-facilitated Ca^{2+} fluctuations.

In Ca^{2+} imaging, U73122 was bath-applied to wild-type round chondrocytes pretreated with or without CNP. Representative recording traces are shown (left panels), and the effects of U73122 are summarized (right bar-graphs). Data represent means ± SEM, and the numbers of cells and mice examined are shown in parentheses in the keys and graph bars, respectively. Significant differences between before and after the U73122 treatment are marked with asterisks (*p<0.05 and **p<0.01 in one-way ANOVA and Tukey's test).

Figure 7

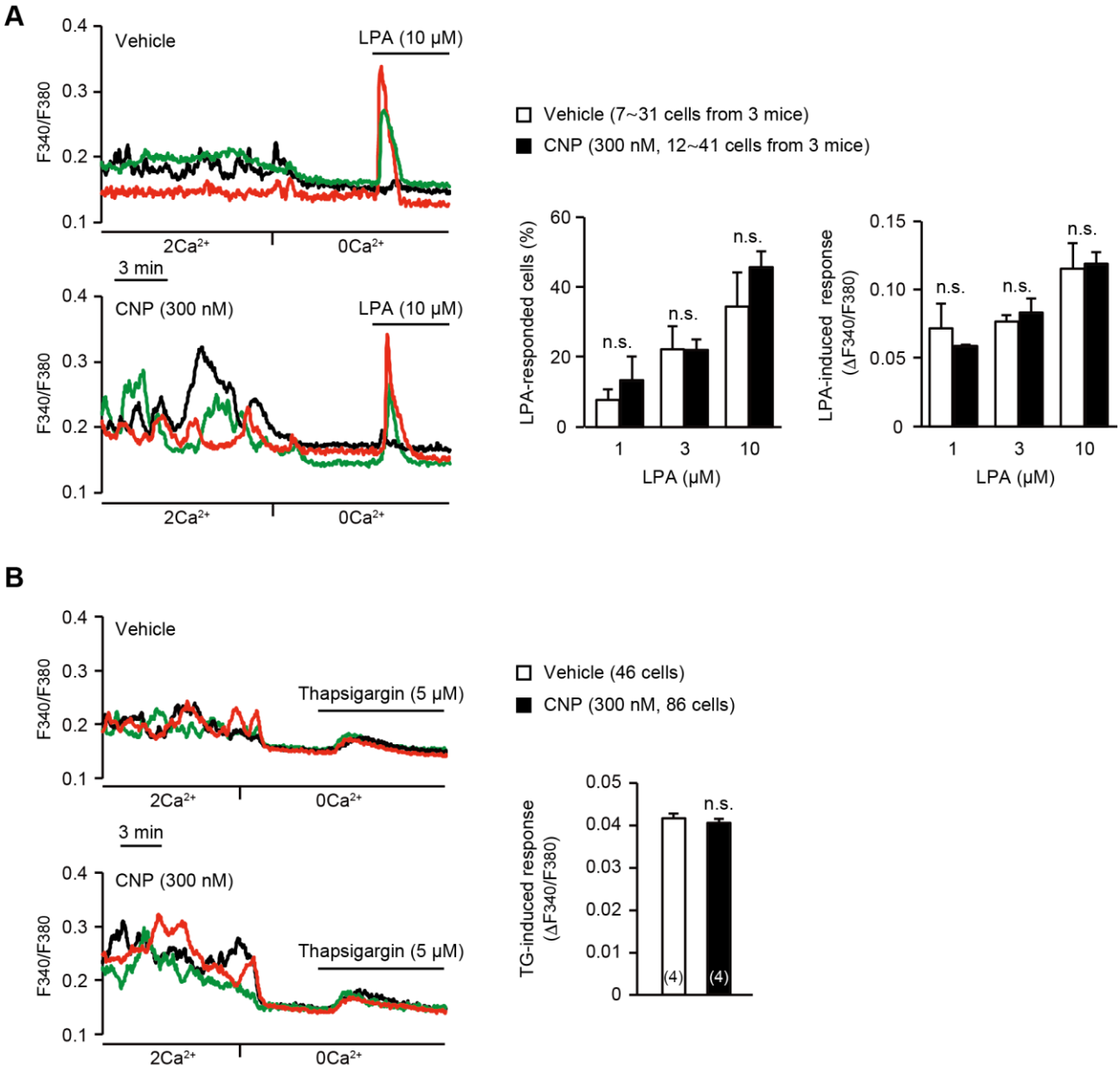

Store Ca^{2+} release in CNP-treated round chondrocytes.

(A) Store Ca^{2+} release triggered by 1-oleoyl lysophosphatidic acid (LPA) in wild-type round chondrocytes pretreated with or without CNP. Representative recording traces are shown (left panels), and LPA-evoked Ca^{2+} responses are summarized (right graphs). Data represent means ± SEM, and the numbers of cells and mice examined are shown in parentheses in the keys and graph bars, respectively. No significant differences were observed between CNP- and vehicle-pretreated groups (one-way ANOVA and Tukey's test). **(B)** Ca^{2+} leak responses evoked by the SERCA pump inhibitor thapsigargin (TG) in wild-type round chondrocytes pretreated with or without CNP. Representative recording traces are shown (left panels), and TG-evoked Ca^{2+} responses are summarized (right bar-graphs). Data represent means ± SEM, and the numbers of cells and mice examined are shown in parentheses in the keys and graph bars, respectively. No significant differences were

observed between CNP- and vehicle-pretreated groups (*t*-test).

CNP induces BK channel-mediated hyperpolarization

To confirm the contribution of activated BK channels to CNP-facilitated Ca^{2+} fluctuations, I conducted confocal imaging using the voltage-dependent dye oxonol VI. In this imaging analysis, depolarization results in the accumulation of the dye into cells, in which the fractional fluorescence intensity, normalized to the maximum intensity monitored in the bath solution containing 100 mM KCl, is thus increased (Figure 8A left panel). The fractional intensity of CNP-pretreated cells was significantly lower than that of non-treated cells in a normal bath solution (Figure 8A middle graph), although both cells exhibited similar intensity shifts in high K^+ bath solutions. Based on the recording data, I prepared a calibration plot for the relationship between the fractional intensity and theoretical membrane potential (Figure 8A right panel). In the tentative linear correlation, resting potentials of -46.4 ± 0.2 and -43.6 ± 0.3 mV were estimated in CNP-treated and non-treated cells, respectively. The estimated potentials closely approximate the reported value from monitoring articular chondrocytes using sharp microelectrodes [23].

In pharmacological assessments, paxilline elevated fractional intensities to the same levels in CNP-and non-treated chondrocytes (Figure 8B). Moreover, NS1619 decreased fractional intensities to the same levels in both cells under 20 mM KCl bathing conditions, which enabled us to reliably

evaluate the reducing intensity shifts (Figure 8C). The oxonol VI imaging data suggested that CNP treatments induce BK channel-mediated hyperpolarization and thus facilitate spontaneous Ca^{2+} fluctuations by enhancing Ca^{2+}-driving forces in growth plate chondrocytes.

Figure 8

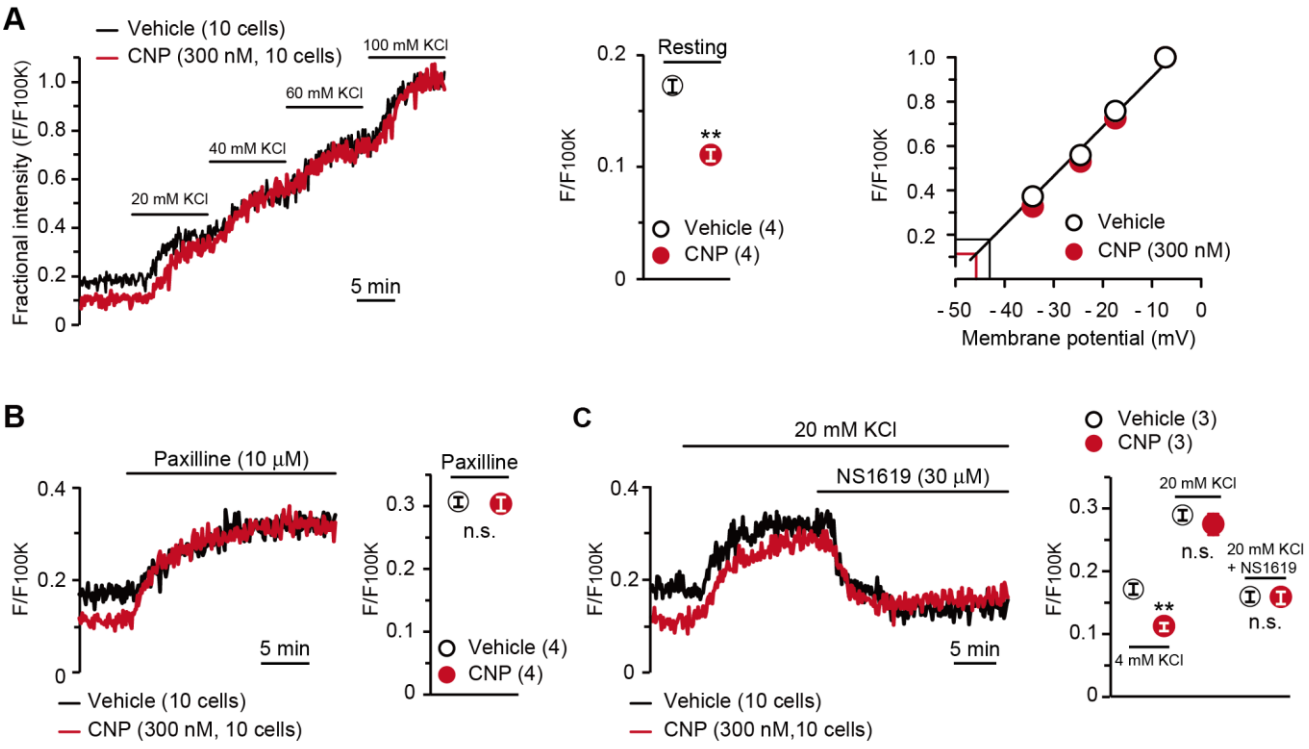

BK channel-mediated hyperpolarization induced by CNP.

(A) Oxonol VI imaging of round chondrocytes pretreated with or without CNP. Wild-type bone slices were pretreated with or without CNP, and then subjected to membrane potential imaging. During contiguous treatments with high-K^+ solutions, cellular fluorescence intensities were monitored and normalized to the maximum value in the 100 mM KCl-containing solution to yield the fractional intensity (left panel). The resting fractional intensities were quantified and statistically analyzed in CNP- and vehicle-pretreated cells (middle graph). For preparing the calibration plot (right panel), the data from ten cells in bathing solutions containing 4 (normal solution), 20, 40, 60 and 100 mM KCl are summarized; red and black lines indicate the estimated resting membrane potentials of CNP- and vehicle-pretreated cells, respectively. **(B)** Effects of the BK channel inhibitor paxilline on resting membrane potential in round chondrocytes. Recording data from ten cells pretreated with or without CNP were averaged (left panel), and the fractional intensities elevated by paxilline are summarized (right graph). **(C)** Effects of the BK channel activator NS1619 on membrane potential in round chondrocytes. Recording data from ten cells pretreated with or without CNP were averaged (left panel), and the fractional intensities in normal, 20 mM KCl and NS1619-containing 20 mM KCl solutions are summarized (right graph). Significant differences between CNP- and vehicle-pretreated cells are indicated by asterisks in **A** (**p<0.01 in t-test) and in **C** (**p<0.01 in one-way ANOVA and Dunn's test). The data are presented as the means ± SEM. with n values indicating the number of examined mice.

CNP enhances TRPM7-mediated Ca^{2+} entry and CaMKII activity

Spontaneous Ca^{2+} fluctuations are predominantly attributed to the intermissive gating of cell-surface TRPM7 channels in growth plate chondrocytes [11]. For pharmacological characterization of TRPM7 channels, FTY720 is used as a typical inhibitor, while NNC550396 is an activator. As reasonably expected, bath application of FTY720 (10 μM) clearly diminished CNP-facilitated Ca^{2+} fluctuations in round chondrocytes (Figure 9A). On the other hand, NNC550396 (30 μM) remarkably facilitated Ca^{2+} fluctuation in non-treated chondrocytes, and this facilitation was preserved in the mutant chondrocytes prepared from chondrocyte-specific *Npr2*-knockout mice (Figure 9B). Therefore, CNP treatments likely facilitate TRPM7-mediated Ca^{2+} influx in growth plate chondrocytes.

TRPM7-mediated Ca^{2+} entry activates CaMKII in growth plate chondrocytes toward bone outgrowth [11], and cellular CaMKII activity can be estimated by immunochemically quantifying its autophosphorylated form. In immunocytochemical analysis, CNP-pretreated growth plate chondrocytes were more decorated with the antibody against phospho-CaMKII than non-treated control cells (Figure 10A). This CNP-facilitated decoration was abolished by the cotreatment of the CaMKII inhibitor KN93 (30 μM). This observation was further confirmed by Western blot analysis; CNP treatments increased the phospho-CaMKII population without affecting total CaMKII content

in the cell lysates prepared from growth plates (Figure 10B). Therefore, CaMKII is likely activated downstream of enhanced TRPM7-mediated Ca^{2+} entry in CNP-treated growth plate chondrocytes.

Figure 9

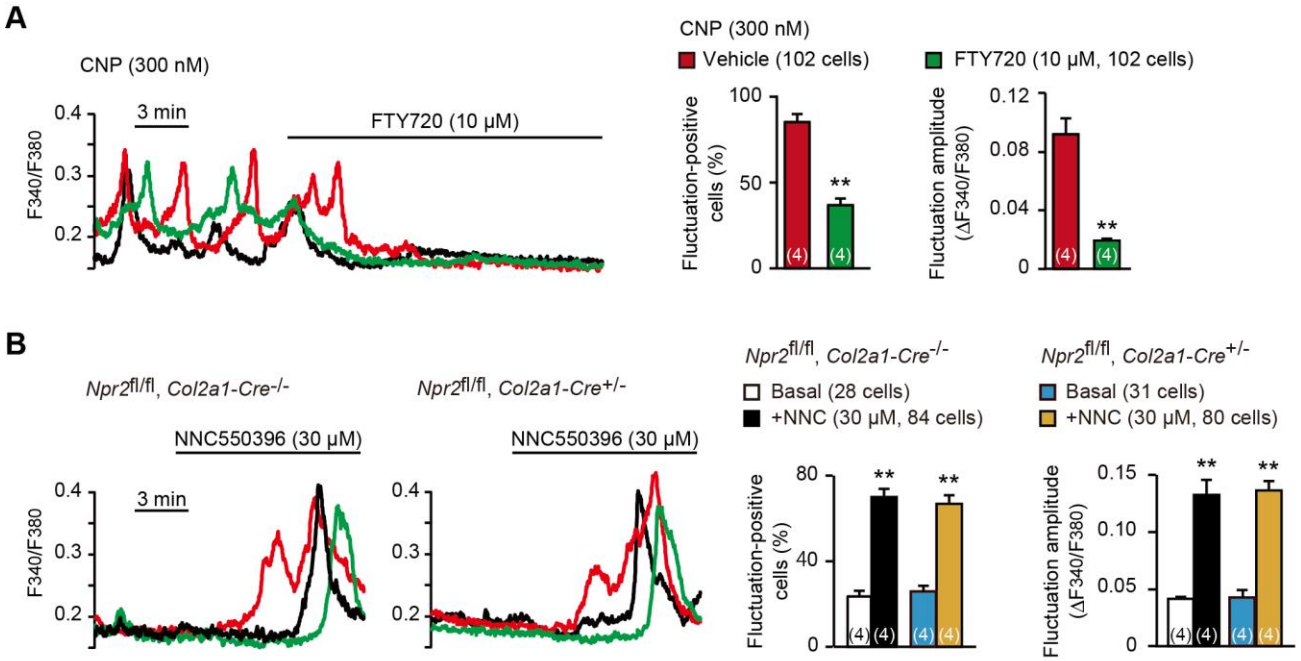

Enhanced TRPM7-mediated Ca^{2+} entry by CNP treatments.

(A) Inhibition of CNP-facilitated Ca^{2+} fluctuations by the TRPM7 inhibitor FTY720 in round chondrocytes. Wild-type bone slices were pretreated with CNP, and then subjected to Ca^{2+} imaging. Representative recording traces are shown (left panel), and the effects of FTY720 are summarized (right graphs). Significant FTY720-induced shifts are marked with asterisks (**p<0.01 in t-test). The data are presented as the means ± SEM. with n values indicating the number of examined mice. **(B)** Ca^{2+} fluctuations facilitated by the TRPM7 channel activator NNC550396 in *Npr2*-deficient round chondrocytes. Bone slices were prepared from the chondrocyte-specific *Npr2*-knockout and control embryos, and NNC550396-induced effects were examined in Ca^{2+} imaging. Representative recording traces are shown (left panels) and the effects of NNC550396 on Ca^{2+} fluctuations are summarized (right graphs). Significant NNC550396-induced shifts in each genotype are marked with asterisks (**p <0.01 in one-way ANOVA and Tukey's test). The data are presented as the means ± SEM. with n values indicating the number of examined mice.

Figure 10

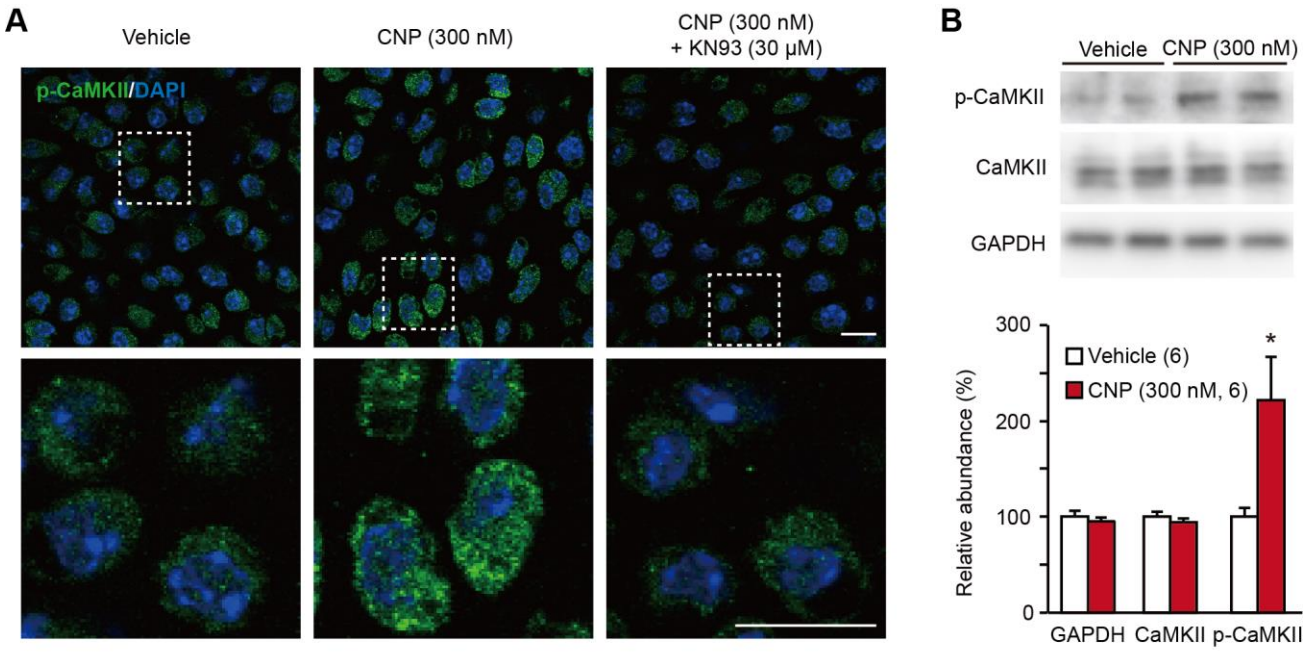

CaMKII activation in CNP-treated round chondrocytes.

(A) Immunohistochemical staining against phospho-CaMKII (p-CaMKII) in round chondrocytes. Wild-type bone slices were pretreated with or without CNP and the CaMKII inhibitor KN93, and then subjected to immunostaining with antibody to p-CaMKII. DAPI (4', 6-diamidino-2- phenylindole) was used for nuclear staining. Lower panels show high-magnification views of white-dotted regions in upper panels (scale bars, 10 μm). **(B)** Immunoblot analysis of total CaMKII and p-CaMKII in growth plate cartilage. Growth plate lysates were prepared from wild-type bone slices pretreated with or without CNP, and subjected to immunoblot analysis with antibodies against total CaMKII and p-CaMKII (upper panel). Glyceraldehyde-3-phosphate dehydrogenase (GAPDH) was also analyzed as a loading control. The immunoreactivities observed were densitometrically quantified and are summarized (lower graph). A significant difference between CNP- and vehicle-pretreatments is marked with an asterisk (*p<0.05 in one-way ANOVA and Tukey's test). The data are presented as the means ± SEM. with n values indicating the number of examined mice.

Pharmacologically activated BK channels facilitate bone outgrowth

Based on the present data from *in vitro* experiments, the novel CNP-signaling route, represented as the NPR2-PKG-BK channel-TRPM7 channel-CaMKII axis, can be proposed in growth plate chondrocytes. I attempted to examine the proposed signaling axis in metatarsal bone culture, a widely used *ex vivo* model system for analyzing bone growth and endochondral ossification [24]. In chondrocyte-specific *Trpm7*-knockout mice (*Trpm7*$^{fl/fl}$, *11Enh*-Cre$^{+/-}$), Cre recombinase is expressed under the control of the collagen type XI gene enhancer and promoter, and thus inactivates the floxed *Trpm7* alleles in cartilage cells [11]. The bone rudiments prepared from control embryos (*Trpm7*$^{fl/fl}$, *11Enh-Cre*$^{-/-}$) regularly elongated during *ex vivo* culture, and their outgrowth was significantly stimulated by the supplementation with CNP (30 nM) into the culture medium (Figure 11A). In contrast, the mutant rudiments prepared from the chondrocyte-specific *Trpm7*-knockout embryos were reduced in initial size and did not respond to the CNP supplementation. Therefore, CNP-facilitated bone outgrowth seems to require TRPM7 channels expressed in growth plate chondrocytes.

In my proposed signaling axis, activated BK channels exert an essential role by converting the chemical signal into the electrical signal. I finally examined the effect of the BK channel activator NS1619 on bone outgrowth (Figure 11B). NS1619 supplementation (30 μM) significantly stimulated

the outgrowth of wild-type bone rudiments. In contrast, under the same culture conditions, no stimulation was detected in the mutant rudiments from the chondrocyte-specific *Trpm7*-deficient embryos. The observations in the bone culture support my conclusion that CNP activates BK channels and thus facilitates TRPM7-mediated Ca^{2+} influx in growth plate chondrocytes, stimulating bone growth.

Figure 11

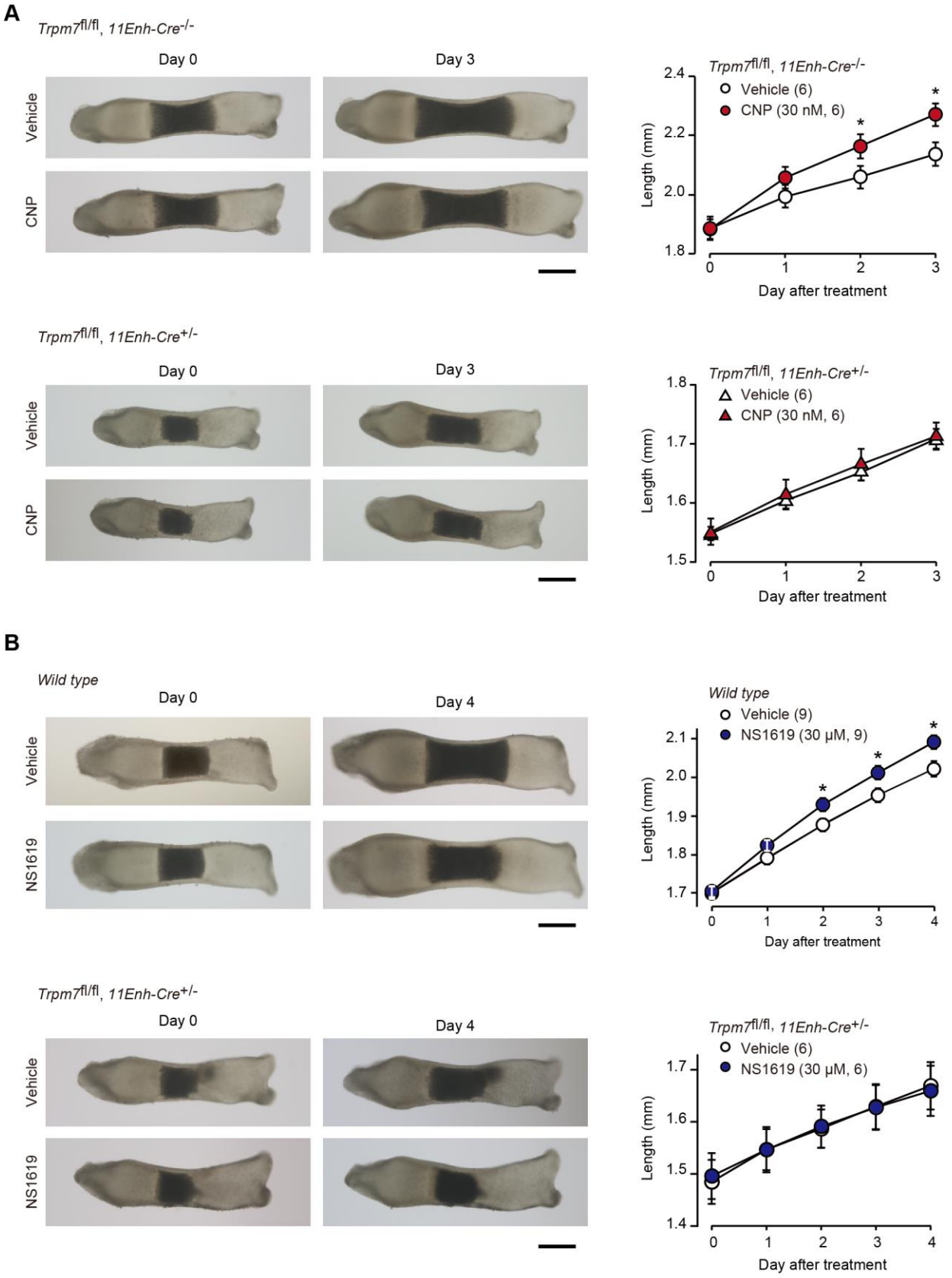
A
Trpm7fl/fl, 11Enh-Cre-/-
Day 0
Day 3
Vehicle
CNP
Trpm7fl/fl, 11Enh-Cre-/-
Vehicle (6)
CNP (30 nM, 6)
Length (mm)
Day after treatment
Trpm7fl/fl, 11Enh-Cre+/-
Day 0
Day 3
Vehicle
CNP
Trpm7fl/fl, 11Enh-Cre+/-
Vehicle (6)
CNP (30 nM, 6)
Length (mm)
Day after treatment
B
Wild type
Day 0
Day 4
Vehicle
NS1619
Wild type
Vehicle (9)
NS1619 (30 µM, 9)
Length (mm)
Day after treatment
Trpm7fl/fl, 11Enh-Cre+/-
Day 0
Day 4
Vehicle
NS1619
Trpm7fl/fl, 11Enh-Cre+/-
Vehicle (6)
NS1619 (30 µM, 6)
Length (mm)
Day after treatment

Contribution of TRPM7 and BK channels to CNP-facilitated bone outgrowth.

(**A**) Loss of CNP-facilitated outgrowth in *Trpm7*-deficient bones. Metatarsal rudiments isolated from the chondrocyte-specific *Trpm7*-knockout (*Trpm7*$^{fl/fl}$, *11Enh-Cre*$^{+/-}$) and control (*Trpm7*$^{fl/fl}$, *11Enh-Cre*$^{-/-}$) embryos were precultured in normal medium for 6 days, and then cultured in medium supplemented with or without CNP for 3 days. Representative images of cultured metatarsals are shown (left panels; scale bar, 0.3 mm), and longitudinal bone outgrowth during the CNP-supplemented period was statistically analyzed in each genotype group (right graphs). Significant CNP-supplemented effects are marked with asterisks (*p<0.05 in t-test). The data are presented as the means ± SEM. with n values indicating the number of examined mice. (**B**) Stimulated bone outgrowth by the BK channel activator NS1619. Metatarsal rudiments isolated from wild-type and the chondrocyte-specific *Trpm7*-knockout embryos were precultured in normal medium for 5 days, and then cultured in medium supplemented with or without NS1619 for 4 days. Representative images of cultured metatarsals are shown (left panels; scale bar, 0.3 mm), and longitudinal bone outgrowth during the NS1619-supplemented period was statistically analyzed in each genotype group (right graphs). A significant NS1619-supplemented effect is marked with asterisks (*p<0.05 in t-test). The data are presented as the means ± SEM. with n values indicating the number of examined mice.

Discussion

I reported that in growth plate chondrocytes, PLC and BK channels maintain autonomic TRPM7-mediated Ca^{2+} fluctuations, which potentiate chondrogenesis and bone growth by activating CaMKII [11]. Based on the present data, together with the previous reports, I proposed a new CNP signaling axis in growth plate chondrocytes (Figure 12A). CNP-induced NPR2 activation elevates cellular cGMP content and thus activates PKG, leading to the phosphorylation of BK channels. The resulting BK channel activation likely induces cellular hyperpolarization to facilitate TRPM7-mediated Ca^{2+} entry by enhancing the Ca^{2+} driving force, leading to CaMKII activation. Therefore, it is likely that CaMKII activity is physiologically regulated by BK channels as a key player of the CNP signaling cascade. In a recent genetic study, several patients carrying loss-of-function mutations in the *KCNMA1* gene encoding BK channel α subunit were characterized by a novel syndromic growth deficiency associated with severe developmental delay, cardiac malformation, bone dysplasia and dysmorphic features [25]. In the *KCNMA1*-mutated disorder, CNP signaling likely fails to facilitate TRPM7-mediated Ca^{2+} fluctuations in growth plate chondrocytes and resulting insufficient Ca^{2+} entry may lead to systemic bone dysplasia associated with stunted growth plate cartilage. On the other hand, the origin of CNP may still be ambiguous in the signaling scheme. Transgenic mice overexpressing CNP in a chondrocyte-specific manner develop a

prominent skeletal overgrowth phenotype, suggesting autocrine CNP signaling [26]. However, several genechip data in public databases indicate that prepro-CNP mRNA is abundantly expressed in the placenta among embryonic tissues (for example, see the records under accession number GSE28277 in NCBI database). Therefore, it may be important to further examine which cell type primarily produces CNP to facilitate bone growth during embryonic development.

From a physiological point of view, it is interesting to note that the proposed CNP signaling axis has clear overlap with the nitric oxide (NO) and ANP/BNP signaling cascades for vascular relaxation [27-29]. In blood vessels, NO is produced by endothelial cells in response to various stimuli including shear stress and acetylcholine, and activates soluble guanylate cyclase in neighboring vascular smooth muscle cells. ANP and BNP are released from the heart in response to pathological stresses, such as atrial distension and pressure overload, and are delivered to activate the receptor guanylate cyclase NPR1 in vascular muscle. In either case, the resulting cGMP elevation followed by PKG activation induces BK channel-mediated hyperpolarization and thus inhibits L-type Ca^{2+} channel gating, leading to vascular dilation due to decreased Ca^{2+} entry into vascular muscle. Therefore, activated BK channels inhibit the voltage-dependent Ca^{2+} influx in vascular muscle cells regarded as excitable cells (Figure 12B). In contrast, activated BK channels reversely stimulate TRPM7-mediated Ca^{2+} entry in growth plate chondrocytes classified as nonexcitable cells, because

the channel activity is voltage-independently maintained by the intrinsic PI turnover rate.

CNP is an effective therapeutic reagent for achondroplasia and divergent short statures [26, 30, 31], and vosoritide, a stable analog of CNP has recently been approved for the treatment of achondroplasia [32]. The proteins contributing to the CNP signaling axis may be new pharmaceutical targets for developing medications; in addition to NPR2, BK and TRPM7 channels are reasonably considered promising targets. Moreover, phosphodiesterase subtypes might be useful targets, although the subtypes responsible for cGMP hydrolysis remain to be identified in growth plate chondrocytes. Chemical compounds specifically targeting the signaling axis defined in this study would be useful drugs for not only clinical treatment of developmental disorders but also artificially modifying body sizes in farm and pet animals.

Figure 12

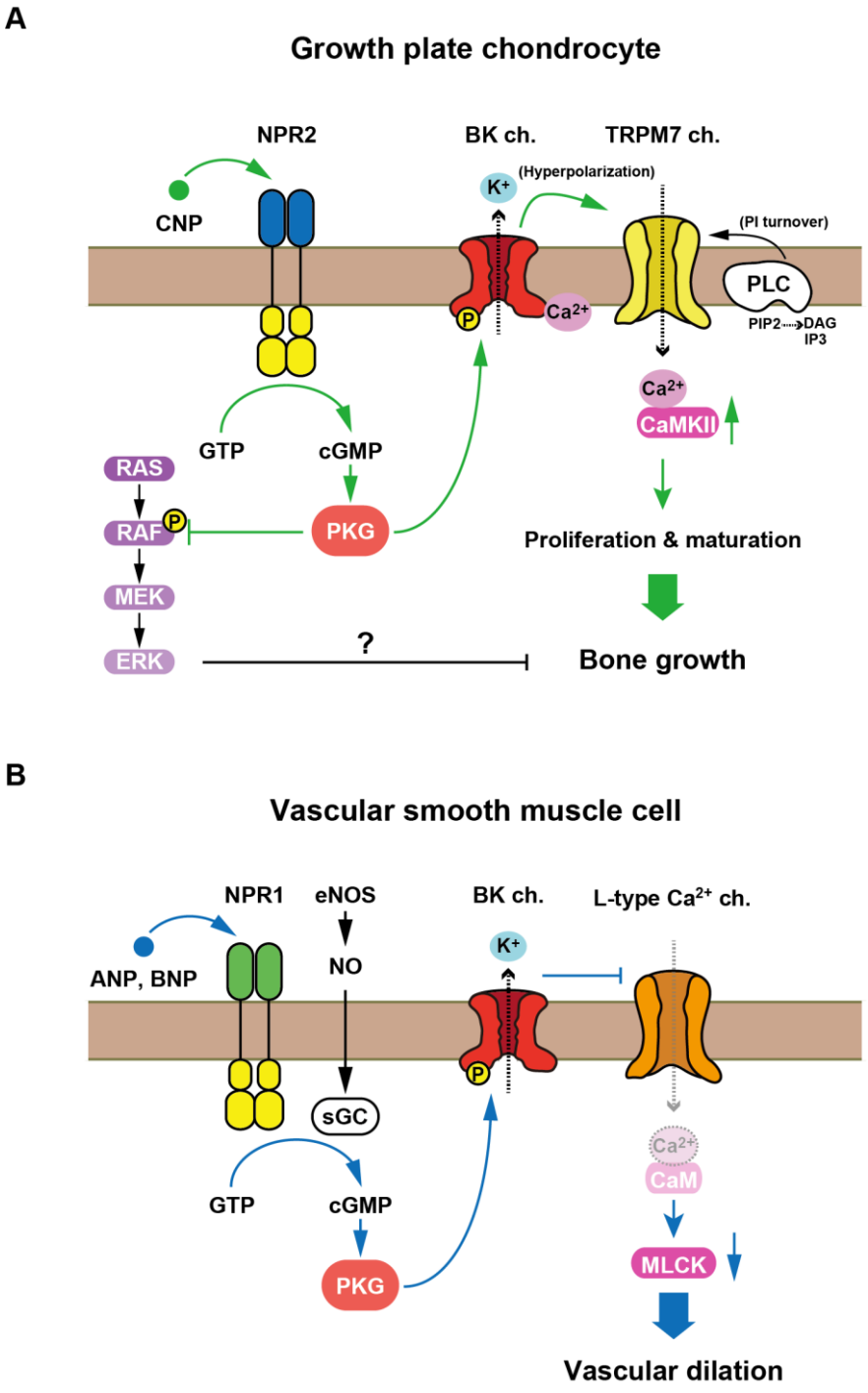

Proposed CNP-evoked signaling in growth plate chondrocytes and its mechanistic similarity to known ANP/BNP and NO signaling in vascular smooth muscle cells.

(A) The schematic diagram representing the NPR2-PKG-BK channel-TRPM7 channel-CaMKII axis proposed as an essential CNP signaling cascade in growth plate chondrocytes. Previous studies proposed that the RAF-MEK-ERK axis is also involved in growth plate CNP signaling [8]. **(B)** The schematic diagram representing the NO- and ANP/BNP-induced relaxation signaling in vascular smooth muscle.

Materials and Methods

Reagents, primers and mice

Reagents and antibodies used in this study are listed in Table 1. Synthetic primers used for RT-PCR analysis and mouse genotyping are listed in Table 2. C57BL mice were used as wild-type mice in this study. Chondrocyte-specific *Trpm7*-knockout mice with C57BL genetic background were generated and genotyped as previously described [11]. Chondrocyte-specific *Npr2*-knockout mice with C57BL background were generated as previously described [12], and I newly designed primers for detecting the *Col2a1-Cre* transgene and the floxed *Npr2* gene in this study (Figure 2). All experiments in this study were conducted with the approval of the Animal Research Committee according to the regulations on animal experimentation at Kyoto University.

Bone slice preparations

Femoral bones were isolated from E17.5 mice and immersed in a physiological salt solution (PSS): (in mM) 150 NaCl, 4 KCl, 1 $MgCl_2$, 2 $CaCl_2$, 5.6 glucose, and 5 HEPES (pH 7.4). Longitudinal bone slices (~40 μm thickness) were prepared using a vibrating microslicer (DTK-1000N, Dosaka EM Co., Japan) as previously described [11].

Ca^{2+} imaging

Fura-2 Ca^{2+} imaging of bone slices was performed as previously described [11]. Briefly, bone slices placed on glass-bottom dishes (Matsunami, Japan) were incubated in PSS containing 15 μM Fura-2 AM for 1 hr at 37°C. For ratiometric imaging, excitation light of 340 and 380 nm was alternately delivered, and emission light of >510 nm was detected by a cooled EM-CCD camera (Model C9100-13; Hamamatsu Photonics, Japan) mounted on an upright fluorescence microscope (DM6 FS, Leica, Germany) using a 40x water-immersion objective (HCX APO L, Leica). In typical measurements, ~30 round chondrocytes were randomly examined in each slice preparation to select the Ca^{2+} fluctuation-positive cells generating spontaneous events (>0.025 in Fura-2 ratio) using commercial software (Leica Application Suite X), and recording traces from the positive cells were then analyzed using Fiji/ImageJ software (US. NIH) for examining Ca^{2+} fluctuation amplitude and frequency. Imaging experiments were performed at room temperature (23-25 °C) and PSS was used as the normal bathing solution. For the pretreatments of CNP, ANP and 8-pCPT-cGMP, bone slices were immersed in PSS with the indicated compound for 1 hr at room temperature after Fura-2 loading.

Membrane potential monitoring

Bone slices were perfused with the PSS containing 200 nM oxonol VI at room temperature and analyzed as previously described [33]. To prepare the calibration plot showing the relationship between the fluorescence intensity and membrane potential, saline solutions containing 20 mM, 40 mM, 60 mM or 100 mM KCl were used as bathing solutions. Fluorescence images with excitation at 559 nm and emission at >606 nm were captured at a sampling rate of ~7.0 s using a confocal laser scanning microscope (FV1000; Olympus).

Immunochemical analysis of CaMKII

Bone slices were pretreated with or without CNP were subjected to immunochemical assessments as previously described [34]. Briefly, for immunohistochemical analysis, bone slices were fixed in 4% paraformaldehyde and treated with 1% hyaluronidase to enhance immunodetection [35, 36]. After blocking with fetal bovine serum-containing solution, bone slices were reacted with primary and Alexa 488-conjugated secondary antibodies and observed with a confocal microscope (FV1000; Olympus). For immunoblot analysis, bone slices were lysed in the buffer containing 4% sodium deoxycholate, 20 mM Tris-HCl (pH 8.8) and a phosphatase inhibitor cocktail (100 mM NaF, 10 mM Na_3PO_4, 1 mM Na_2VO_3 and 20 mM β-glycerophosphate). The resulting lysate proteins were electrophoresed on SDS-polyacrylamide gels and electroblotted onto nylon membranes for

immunodetection using primary and HRP-conjugated secondary antibodies. Antigen proteins were visualized using a chemiluminescence reagent and image analyzer (Amersham Imager 600, Cytiva). The immunoreactivities yielded were quantitatively analyzed by means of Fiji/ImageJ software.

Metatarsal organ culture

Metatarsal bone rudiments were cultured as previously described [24]. Briefly, the three central metatarsal rudiments were dissected from E15.5 mice and cultured in αMEM containing 5 μg/ml ascorbic acid, 1 mM β-glycerophosphate pentahydrate, 100 units/ml penicillin, 100 μg/ml streptomycin and 0.2% bovine serum albumin (fatty acid free). The explants were analyzed under a photomicroscope (BZ-X710, Keyence, Japan) for size measurements using Fiji/ImageJ software.

Gene expression analysis

Quantitative RT-PCR analysis was performed as previously described [37]. Total RNA was prepared from mouse tissues using a commercial reagent (Isogen) and reverse-transcribed using a commercial kit (ReverTra ACE qPCR-RT kit). The resulting cDNAs were examined by real-time PCR (LightCycler 480 II, Roche), and the cycle threshold was determined from the amplification curve as an index for relative mRNA content in each reaction.

Quantification and statistical analysis

All data obtained are presented as the means ± SEM. with *n* values indicating the number of examined mice. Student *t*-test and ANOVA were used for two-group and multiple group comparisons, respectively (Prism 7, GraphPad Software Inc.): $p<0.05$ was considered to be statistically significant.

Table 1. Chemical reagents for pharmacological analysis

Reagent/Resource	Source	Identifier
Antibodies		
Anti-phospho-CaMKII (Thr 286)	Cell Signaling Technology	Cat#12716; RRID: AB_2713889
Anti-CaMKII	Abcam	Cat#EP1829Y; RRID: AB_868641
Anti-GAPDH	Sigma-Aldrich	Cat#G9545; RRID: AB_796208
Anti-rabbit IgG-HRP	Santa Cruz	Cat#sc-2357; RRID; AB_628497
Anti-rabbit Alexa Flour 488	Invitrogen	Cat#A-11008; RRID: AB_143165
Chemicals		
Amersham ECL Prime Western Blotting Detection	Cytiva	Cat#RPN2232
ANP (Human, 1-28)	Peptide Institute	Cat#4135
CNP-22 (Human)	Peptide Institute	Cat#4229
FTY720	Sigma-Aldrich	SML0700; CAS: 162359-56-0
Fura-2AM	Dojindo	F025; CAS: 108964-32-5
Hyaluronidase from sheep testes	Sigma-Aldrich	H2126; CAS: 37326-33-3
ISOGEN	NipponGene	Cat#319-90211
KN93	Wako	115-00641; CAS: 139298-40-1
KT5823	Cayman Chemical	10010965; CAS: 126643-37-6
NNC 550396 dihydrochloride	Tocris Bioscience	2268; CAS: 357400-13-6
NS1619	Sigma-Aldrich	N170; CAS: 153587-01-0
1-oleoyl lysophosphatidic acid	Cayman Chemical	62215; CAS: 325465-93-8
Oxonol VI	Sigma-Aldrich	75926; CAS: 64724-75-0
Paxilline	Tocris Bioscience	2006; CAS: 57186-25-1
8-pCPT-cGMP	Biolog	C009; CAS: 51239-26-0
ReverTra Ace® qPCR RT Master Mix with gDNA	TOYOBO	Cat#FSQ-301
Thapsigargin	Nacalai Tesque	33637-31; CAS: 67526-95-8
U73122	Sigma-Aldrich	U6756; CAS: 112648-68-7

Table 2. Primers used for PCR analysis

Npr1	For AACAAGGAGAACAGCAGCAAC Rev TATCAAATGCCTCAGCCTGGA	***Npr2***	For GGCCCCATCCCTGATGAAC Rev CCTGGTACCCCCTTCCTGTA
Npr3	For GGTATGGGGACTTCTCTGTG Rev TCTGGTCTCATCTAGTCTCA	***FlFor***	GTAACCTGGGTAGACTAGTTGTTGG
DelFor	TGTTATTTTGTGAGATGACG	***Rev***	ATGGTGGAGGAGGTCTTTAATTCC
Col2a1-Cre	For CGTTGTGAGTTGGATAGTTG Rev CATTGCTGTCACTTGGTCGT	***Prkg1***	For ATGGACTTTTTGTGGGACTC Rev GGTTTTCATTGGATCTGGGC
Prkg2	For TTGCGGAAGAAAATGATGTCG Rev GAATGGGGAGGTTGAGGAGAA	***Kcnma1***	For AATGCACTTCGAGGAGGCTA Rev CTCAGCCGGTAAATTCCAAA
Kcnmb1	For ACAACTGTGCTGCCCCTCTA Rev CACTGTTGGTTTTGATCCCG	***Kcnmb2***	For TCAGGAGACACCAACACTTC Rev AGTTAGTTTCACCATAGCAA
Kcnmb3	For GTGGATGACGGGCTGGACTT Rev GCACTTGGGGTTGGTCCTGA	***Kcnmb4***	For CTCCTGACCAACCCCAAGTG Rev TAAAATAGCAAGTGAATGGC
Kcnn1	For TCAAAAATGCTGCTGCAAAC Rev TCGTTCACCTTCCCTTGTTC	***Kcnn2***	For GATCTGGCAAAGACCCAGAA Rev GAAGTCCCTTTGCTGCTGTC
Kcnn3	For ACTTCAACACCCGATTCGTC Rev GGAAAGGAACGTGATGGAGA	***Kcnn4***	For GGCACCTCACAGACACACTG Rev TTTCTCCGCCTTGTTGAACT
Plcb1	For CCCAAGTTGCGTGAACTTCT Rev GTTGCCAAGCTGAAAACCTC	***Plcb2***	For ACATCCAGGAAGTGGTCCAG Rev CGCACCGACTCCTTTACTTC
Plcb3	For CAGGCCAGCACAGAGACATA Rev AGGATGCTGGCAATCAAATC	***Plcg1***	For AACGCTTTGAGGACTGGAGA Rev CTCCTCAATCTCTCGCAAGG
Plcg2	For AACCCCAACCCACACGAGTC Rev AATGTTTCACCTTGCCCCTG	***Trpm7***	For ATTGCTTAGTTTTGGTGTTC Rev GATTGTCGGGAGAGTGGAGT
Camk2a	For CACCACCATTGAGGACGAAG Rev GGTTCAAAGGCTGTCATTCC	***Camk2b***	For AAGCAGATGGAGTCAAGCC Rev TGCTGTCGGAAGATTCCAGG
Camk2d	For GATAAACAACAAAGCCAACG Rev GTAAGCCTCAAAGTCCCCAT	***Camk2g***	For CAAGAACAGCAAGCCTATCC Rev CCTCTGACTGACTGGTGCGA
Pde2a	For ATCTTTGACCACTTCTCTCG Rev CATAACCCACTTCAGCCATC	***Pde3a***	For AACTATACCTGCTCGGACTC Rev TTCGTGCGGCTTTATGCTGG
Pde3b	For ATTCCAAAGCAGAGGTCATC Rev GTTAGAGAGCCAGCAGACAC	***Pde5a***	For GACCCTTGCGTTGCTCATTG Rev TGATGGAGTGACAGTACAGC
Pde6a	For AACCCACCCGCTGACCACTG Rev CTCTTCCTTCTTGTTGACGA	***Pde6b***	For TCCGGGCCTATCTAAACTGC Rev AGAAGACAATTTCCCGGCCAT
Pde6c	For TTGCTCAGGAAATGGTTATG Rev GAAACAGAACTCGTACAGGT	***Pde6d***	For CCCAAGAAAATCCTCAAGTG Rev ACAAAGCCAAACTCGAAGAA
Pde6g	For AAGGGTGAGATTCGGTCAGC Rev TCATCCCCAAACCCTTGCAC	***Pde6h***	For GGCAGACTCGACAGTTCAAGA Rev CTCCAGATGGCTGAACGCT
Pde10a	For CATCCGCAAAGCCATCATCG Rev TCTCATCACCCTCAGCCCAG	***Lpar1***	For GCTTGGTGCCTTTATTGTCT Rev GGTAGGAGTAGATGATGGGG
Lpar2	For AGTGTGCTGGTATTGCTGAC Rev TTTGATGGAGAGCCTGGCAG	***Lpar3***	For ACTTTCCCTTCTACTACCTG Rev GTCTTTCCACAGCAATAACC
Lpar4	For CCTCAGTGGTGGTATTTCAG Rev CACAGAAGAACAAGAAACAT	***Lpar5***	For AACACGACTTCTACCAACAG Rev AAGACCCAGAGAGCCAGAGC
Lpar6	For TACTTTGCCATTTCGGATTT Rev GCACTTCCTCCCATCACTGT	***Atp2a1***	For CAAAACAGGGACCCTCACCA Rev GCCAGTGATGGAGAACTCGT
Atp2a2	For AAACCAGATGTCCGTGTGCA Rev TGATGGCACTTCACTGGCTT	***Atp2a3***	For CCTCGGTCATCTGCTCTGAC Rev CGTGGTACCCGAAATGGTGA
Pln	For TACCTCACTCGCTCGGCTAT Rev TGACGGAGTGCTCGGCTTTA	***Pthlh***	For CTCCCAACACCAAAAACCAC Rev GCTTGCCTTTCTTCTTCTTC
Col10a1	For CAAGCCAGGCTATGGAAGTC Rev AGCTGGGCCAATATCTCCTT	***Col2a1***	For CACACTGGTAAGTGGGGCAAGACCG Rev GGATTGTGTTGTTTCAGGGTTCGGG
18S	For AGACAAATCGCTCCACCAAC Rev CTCAACACGGGAAACCTCAC	***Actb***	For CATCCGTAAAGACCTCTATGCCAAC Rev ATGGAGCCACCGATCCACA
Gapdh	For TGTGTCCGTCGTGGATCTGA Rev TTGCTGTTGAAGTCGCAGGAG		

References

1. Berendsen, A.D., and Olsen, B.R. (2015). Bone development. *Bone.* 80, 14-18.
2. Nakao, K., Itoh, H., Saito, Y., Mukoyama, M., and Ogawa, Y. (1996). The natriuretic peptide family. *Curr Opin Nephrol Hypertens.* 5, 4-11.
3. Wit, J.M., and Camacho Hübner, C. (2011). Endocrine regulation of longitudinal bone growth. *Endocr Dev.* 21, 30-41.
4. Peake, N.J., Hobbs, A.J., Pingguan-Murphy, B., Salter, D.M., Berenbaum, F., and Chowdhury, T.T. (2014). Role of C-type natriuretic peptide signalling in maintaining cartilage and bone function. *Osteoarthritis Cartilage.* 22, 1800-1807.
5. Vasques, G.A., Arnhold, I.J.P., and Jorge, A.A.L. (2014). Role of the natriuretic peptide system in normal growth and growth disorders. *Horm Res Paediatr.* 82, 222-229.
6. Wit, J.M., Oostdijk, W., Losekoot, M., van Duyvenvoorde, H.A., Ruivenkamp, C.A.L., and Kant, S.G. (2016). MECHANISMS IN ENDOCRINOLOGY: Novel genetic causes of short stature. *Eur J Endocrinol.* 174, R145-R173.
7. Savarirayan, R., Tofts, L., Irving, M., Wilcox, W., Bacino, C.A., Hoover-Fong, J., Ullot Font, R., Harmatz, P., Rutsch, F., Bober, M.B., et al. (2020). Once-daily, subcutaneous vosoritide therapy in children with achondroplasia: a randomised, double-blind, phase 3, placebo-controlled, multicentre trial. *Lancet.* 396, 684-692.
8. Krejci, P., Masri, B., Fontaine, V., Mekikian, P.B., Weis, M., Prats, H., and Wilcox, W.R. (2005). Interaction of fibroblast growth factor and C-natriuretic peptide signaling in regulation of chondrocyte proliferation and extracellular matrix homeostasis. *J Cell Sci.* 118, 5089-5100.
9. Kawasaki, Y., Kugimiya, F., Chikuda, H., Kamekura, S., Ikeda, T., Kawamura, N., Saito, T., Shinoda, Y., Higashikawa, A., Yano, F., et al. (2008). Phosphorylation of GSK-3β by cGMP-dependent protein kinase II promotes hypertrophic differentiation of murine chondrocytes. *J Clin Invest*. 118, 2506-2515.
10. Fleig, A., and Chubanov, V. (2014). Trpm7. *Handb Exp Pharmacol.* 222, 521-546.
11. Qian, N., Ichimura, A., Takei, D., Sakaguchi, R., Kitani, A., Nagaoka, R., Tomizawa, M., Miyazaki, Y., Miyachi, H., Numata, T., et al. (2019). TRPM7 channels mediate spontaneous Ca^{2+} fluctuations in growth plate chondrocytes that promote bone development *Sci Signal.* 12, eaaw4847.
12. Nakao, K., Osawa, K., Yasoda, A., Yamanaka, S., Fujii, T., Kondo, E., Koyama, N., Kanamoto, N., Miura, M., Kuwahara, K., et al. (2015). The local CNP/GC-B system in

growth plate is responsible for physiological endochondral bone growth. *Sci Rep.* 5, 10554.

13. De-Li, D., Peng, Y., Bao-Feng, Y., and Wen-Hui, W. (2008). Hydrogen peroxide stimulates the Ca^{2+}-activated big-conductance K channels (BK) through cGMP signaling pathway in cultured human endothelial cells. *Cell Physiol Biochem.* 22, 119-126.
14. Fukao, M., Mason, H.S., Britton, F.C., Kenyon, J.L., Horowitz, B., and Keef, K.D. (1999). Cyclic GMP-dependent protein kinase activates cloned BK Ca channels expressed in mammalian cells by direct phosphorylation at serine 1072. *J Biol Chem.* 274, 10927-10935.
15. White, R.E., Kryman, J.P., El-Mowafy, A.M., Han, G., and Carrier, G.O. (2000). cAMP-dependent vasodilators cross-activate the cGMP-dependent protein kinase to stimulate BK(Ca) channel activity in coronary artery smooth muscle cells. *Circ Res.* 86, 897-905.
16. Guo, J.Y., Zhang, M.H., Jiang, J.Z., Piao, L.H., Fang, X.S., Jin, Z., and Cai, Y.L. (2018). The role of CNP-mediated PKG/PKA-PLCβ pathway in diabetes-induced gastric motility disorder. *Peptides.* 110, 47-55.
17. Huang, J., Zhou, H., Mahavadi, S., Sriwai, W., and Murthy, K.S. (2007). Inhibition of Gαq-dependent PLC-β1 activity by PKG and PKA is mediated by phosphorylation of RGS4 and GRK2. *Am J Physiol Cell Physiol.* 292, C200-C208.
18. Nalli, A.D., Kumar, D.P., Al-Shboul, O., Mahavadi, S., Kuemmerle, J.F., Grider, J.R., and Murthy, K.S. (2014). Regulation of Gβγi-dependent PLC-β3 activity in smooth muscle: Inhibitory phosphorylation of PLC-β3 by PKA and PKG and stimulatory phosphorylation of Gαi-GTPase-activating protein RGS2 by PKG. *Cell Biochem Biophys.* 70, 867-880.
19. Xia, C., Bao, Z., Yue, C., Sanborn, B.M., and Liu, M. (2001). Phosphorylation and regulation of G-protein-activated phospholipase C-β3 by cGMP-dependent protein kinases. *J Biol Chem.* 276, 19770-19777.
20. Bibli, S.I., Andreadou, I., Chatzianastasiou, A., Tzimas, C., Sanoudou, D., Kranias, E., Brouckaert, P., Coletta, C., Szabo, C., Kremastinos, D.T., et al. (2015). Cardioprotection by H2S engages a cGMP-dependent protein kinase G/phospholamban pathway. *Cardiovasc Res.* 106, 432-442.
21. Luc, R., Franz, H., and Rik, C. (1988). Cyclic GMP-dependent protein kinase phosphorylates phospholamban in isolated sarcoplasmic reticulum from cardiac and smooth muscle. *Biochem J.* 252, 269-273.
22. Lalli, M.J., Shimizu, S., Sutliff, R.L., Kranias, E.G., and Paul, R.J. (1999). $[Ca^{2+}]_i$ homeostasis and cyclic nucleotide relaxation in aorta of phospholamban-deficient mice. *Am J Physiol.* 277, H963-970.
23. Clark, R.B., Hatano, N., Kondo, C., Belke, D.D., Brown, B.S., Kumar, S., Votta, B.J., and Giles, W.R. (2014). Voltage-gated K^+ currents in mouse articular chondrocytes regulate

membrane potential. *Channels.* 4, 179-191.

24. Houston, D.A., Staines, K.A., MacRae, V.E., and Farquharson, C. (2016). Culture of murine embryonic metatarsals: A physiological model of endochondral ossification. *J Vis Exp.*, e54978.
25. Liang, L., Li, X., Moutton, S., Schrier Vergano, S.A., Cogné, B., Saint-Martin, A., Hurst, A.C.E., Hu, Y., Bodamer, O., Thevenon, J., et al. (2019). De novo loss-of-function KCNMA1 variants are associated with a new multiple malformation syndrome and a broad spectrum of developmental and neurological phenotypes. *Hum Mol Genet.* 28, 2937-2951.
26. Yasoda, A., Komatsu, Y., Chusho, H., Miyazawa, T., Ozasa, A., Miura, M., Kurihara, T., Rogi, T., Tanaka, S., Suda, M., et al. (2004). Overexpression of CNP in chondrocytes rescues achondroplasia through a MAPK-dependent pathway. *Nat Med.* 10, 80-86.
27. Martel, G., Hamet, P., and Tremblay, J. (2009). Central role of guanylyl cyclase in natriuretic peptide signaling in hypertension and metabolic syndrome. *Mol Cell Biochem.* 334, 53-65.
28. Zois, N.E., Bartels, E.D., Hunter, I., Kousholt, B.S., Olsen, L.H., and Goetze, J.P. (2014). Natriuretic peptides in cardiometabolic regulation and disease. *Nat Rev Cardiol.* 11, 403-412.
29. Kubacka, M., Kotańska, M., Kazek, G., Waszkielewicz, A.M., Marona, H., Filipek, B., and Mogilski, S. (2018). Involvement of the NO/sGC/cGMP/K^+ channels pathway in vascular relaxation evoked by two non-quinazoline α1-adrenoceptor antagonists. *Biomed Pharmacother.* 103, 157-166.
30. Ueda, Y., Yasoda, A., Yamashita, Y., Kanai, Y., Hirota, K., Yamauchi, I., Kondo, E., Sakane, Y., Yamanaka, S., Nakao, K., et al. (2016). C-type natriuretic peptide restores impaired skeletal growth in a murine model of glucocorticoid-induced growth retardation. *Bone.* 92, 157-167.
31. Yamashita, T., Fujii, T., Yamauchi, I., Ueda, Y., Hirota, K., Kanai, Y., Yasoda, A., and Inagaki, N. (2020). C-Type natriuretic peptide restores growth impairment under enzyme replacement in mice with mucopolysaccharidosis VII. *Endocrinology.* 161, bqaa008.
32. Fafilek, B., Bosakova, M., and Krejci, P. (2021). Expanding horizons of achondroplasia treatment: current options and future developments. *Osteoarthritis Cartilage.* S1063-4584, 00980-00988.
33. Yamazaki, D., Tabara, Y., Kita, S., Hanada, H., Komazaki, S., Naitou, D., Mishima, A., Nishi, M., Yamamura, H., Yamamoto, S., et al. (2011). TRIC-A channels in vascular smooth muscle contribute to blood pressure maintenance. *Cell Metab.* 14, 231-241.
34. Li, Y., Ahrens, M.J., Wu, A., Liu, J., and Dudley, A.T. (2011). Calcium/calmodulin-dependent protein kinase II activity regulates the proliferative potential of growth plate chondrocytes. *Development.* 138, 359-370.

35. Ahrens, M.J., and Dudley, A.T. (2011). Chemical pretreatment of growth plate cartilage increases immunofluorescence sensitivity. *J Histochem Cytochem.* 59, 408-418.
36. Mouser, V.H.M., Melchels, F.P.W., Visser, J., Dhert, W.J.A., Gawlitta, D., and Malda, J. (2016). Yield stress determines bioprintability of hydrogels based on gelatin-methacryloyl and gellan gum for cartilage bioprinting. *Biofabrication.* 8, 035003.
37. Chengzhu, Z., Ichimura, A., Qian, N., Iida, T., Yamazaki, D., Noma, N., Asagiri, M., Yamamoto, K., Komazaki, S., Sato, C., et al. (2016). Mice lacking the intracellular cation channel TRIC-B have compromised collagen production and impaired bone mineralization. *Sci Signal.* 9, ra49.

Publication list

Miyazaki, Y., Ichimura, A., Kitayama, R., Okamoto, N., Yasue, T., Liu, F., Ueda, Y., Yamauchi, I., Hakata, T., Nakao, K. Kakizawa, S., Nishi, M.,Mori, Y., Akiyama, H., Nakao, K. and Takeshima, H. (2021). C-type natriuretic peptide facilitates autonomic Ca^{2+} entry in growth plate chondrocytes for stimulating bone growth. *bioRxiv.*

Reference Thesis

Miyazaki, Y., Ichimura, A., Sato, S., Fujii, T., Oishi, S., Sakai, H. and Takeshima, H. (2018). The natural flavonoid myricetin inhibits gastric H^+, K^+-ATPase. *Eur J Pharmacol.* 820, 217-221.

Qian, N., Ichimura, A., Takei, D., Sakaguchi, R., Kitani, A., Nagaoka, R., Tomizawa, M., Miyazaki, Y., Miyachi, H., Numata, T., Kakizawa, S., Nishi, M., Yasuo Mori, Y. and Takeshima, H. TRPM7 channels mediate spontaneous Ca^{2+} fluctuations in growth plate chondrocytes that promote bone development. (2019). *Sci Signal.* 12, eaaw4847.

Acknowledgments

I appreciate gratefully to Professor Hiroshi Takeshima, Graduate School of Pharmaceutical Science, Kyoto University for his immediate guidance through this paper. I also appreciate to Assistant Professor Atsuhiko Ichimura, Graduate School of Pharmaceutical Science, Kyoto University for his immediate guidance and encouragement through the course of this work. My appreciation is also given to Associate Professor Sho Kakizawa and, Dr. Miyuki Nishi, Graduate School of Pharmaceutical Science, Kyoto University, Dr. Hiromu Itoh, Kurashiki Central Hospital, Dr. Kazuwa Nakao, Dr. Kazumasa Nakao, Dr. Ichiro Yamauchi and Dr. Yohei Ueda, Graduate School of Medicine, Dr. Yasuo Mori, Graduate School of Engineering, Kyoto Univeristy, Dr. Haruhiko Akiyama, Graduate School of Medicine, Gifu University. I thank Mr. Hitoshi Miyachi, Ms. Satsuki Kitano, and Mr. Jun Matsushita for mouse *in vitro* fertilization. I appreciate to the late Tetsuro Fujita and his family or persons concerned for giving Fujita Jinsei Scholarship. And I express my acknowledgment to co-workers of my research group: Mr. Ryo Kitayama, Mr. Naoki Okamoto, Mr. Tomoki Yasue, Mr. Feng Liu, Ms. Yitong Wang, Mr. Takaaki Kawabe and Mr. Hiroki Nagatomo. I also appreciate to the members of the department of Biological Chemistry, Graduate School of Pharmaceutical Science, Kyoto University for their continuous encouragement helpful discussions and technical supports. I also appreciate to my friends. Lastly, I would like to express my gratitude to my parents and brother for mental encouragement and persistent understanding.